c2

Copy 6
RM L56D03

NACA RM L56D03

RESEARCH MEMORANDUM

LOW-SPEED WIND-TUNNEL RESULTS FOR A THIN ASPECT-RATIO-1.85 POINTED-WING—FUSELAGE MODEL WITH DOUBLE SLOTTED FLAPS

By Albert E. Brown

Langley Aeronautical Laboratory
Langley Field, Va.

CLASSIFICATION CHANGED

UNCLASSIFIED

To NACA Res abs effective

By authority of RN-126 Date Apr. 15, 1958

AMT 5-13-58

NATIONAL ADVISORY COMMITTEE FOR AERONAUTICS

WASHINGTON

July 27, 1956

NATIONAL ADVISORY COMMITTEE FOR AERONAUTICS

RESEARCH MEMORANDUM

LOW-SPEED WIND-TUNNEL RESULTS FOR A THIN ASPECT-RATIO-1.85 POINTED-WING—FUSELAGE MODEL WITH DOUBLE SLOTTED FLAPS

By Albert E. Brown

SUMMARY

Results are presented of a wind-tunnel investigation at low speeds of a thin aspect-ratio-1.85 pointed-wing—fuselage model equipped with double slotted flaps, including the effects of a straight and a delta horizontal tail on the static longitudinal stability and the effect of a delta vertical tail on the static lateral stability. The results indicated that flap effectiveness increased with increase of flap deflection up to 52.5°. For flap deflections greater than 52.5°, flap effectiveness decreased with increase of flap deflection. With a flap deflection of 52.5°, the lift coefficient at an angle of attack of 0° was 0.66 and the maximum lift coefficient was 1.53. Most of the lift-coefficient increment at an angle of attack of 0° held throughout the angle-of-attack range to near stall. For longitudinal stability of the model with the double slotted flaps deflected, the satisfactory location for a straight or delta horizontal tail was rearward and below the wing chord line extended. However, the straight horizontal tail studied would not provide longitudinal trim. The delta vertical tail provided static-directional stability of the model except at high lift coefficients and generally increased the effective dihedral.

INTRODUCTION

Previous investigations (refs. 1 to 4) have shown that large increments of trim lift coefficient can be obtained on delta-wing airplanes by use of double slotted flaps and that static longitudinal stability can be maintained up through the stall by the use of a properly located horizontal tail. The large increments of lift coefficient were limited to the low and moderate angle-of-attack range and only relatively small gains in maximum lift coefficient were obtained because of the reduction in flap effectiveness at angles of attack near the stall. Shifting the hinge line of the double slotted flaps to the delta-wing trailing edge

[redacted]

(extended double slotted flaps) resulted in a configuration in which the flap effectiveness held to angles of attack near the stall (ref. 5). The present investigation was made to determine whether the attainment of flap effectiveness through the angle-of-attack range such as that of reference 5 might be obtained on an aspect-ratio-1.85 pointed-wing plan form with double slotted flaps. Less rearward movement of the flap would be necessary for this configuration than for that of reference 5, and thus less mechanical complication and less diving moment for a given lift-coefficient result. The hinge line of the sweptforward trailing-edge double slotted flap of the present investigation was along the 83 percent chord line which has a sweep of -3.4°. The hinge line of the constant-chord extended double slotted flap of reference 5 was unswept. Results of high-speed investigations made on a pointed wing with flap controls having an unswept hinge line are presented in reference 6.

Included in the investigation were the effects of a delta and a straight horizontal tail on the longitudinal stability and control characteristics of the pointed wing with double slotted flaps. Both tails had approximately the same variation of lift with angle of attack.

In order to make a preliminary evaluation of the static lateral stability of the model, a few tests were made with and without a delta vertical tail at angles of sideslip of $\pm 5^{\circ}$ through the lift-coefficient range.

COEFFICIENTS AND SYMBOLS

The results of the tests are presented as standard coefficients of forces and moments about the stability axes. The positive directions of forces, moments, and angles are shown in figure 1. All moments are referred to the quarter-chord point of the wing mean aerodynamic chord projected on the plane of symmetry as shown in figure 2(a). The coefficients and symbols are defined as follows:

C_L lift coefficient, $\frac{\text{Lift}}{qS}$

C_D drag coefficient, $\frac{\text{Drag}}{qS}$

C_m pitching-moment coefficient, $\frac{\text{Pitching moment}}{qS\bar{c}}$

C_l rolling-moment coefficient, $\frac{\text{Rolling moment}}{qSb}$

C_n yawing-moment coefficient, $\frac{\text{Yawing moment}}{qSb}$

C_Y	lateral-force coefficient, $\frac{\text{Lateral force}}{qS}$
C_{l_β}	variation of rolling moment with sideslip per degree, $\partial C_l/\partial\beta$, measured between $\beta = \pm 5^\circ$
C_{n_β}	variation of yawing moment with sideslip per degree, $\partial C_n/\partial\beta$, measured between $\beta = \pm 5^\circ$
C_{Y_β}	variation of lateral force with sideslip per degree, $\partial C_Y/\partial\beta$, measured between $\beta = \pm 5^\circ$
q	free-stream dynamic pressure, $\frac{1}{2}\rho V^2$, lb/sq ft
S	wing area, 8.63 sq ft
$\bar{c}$	wing mean aerodynamic chord, 2.88 ft, $\frac{2}{S}\int_0^{b/2} c^2 dy$ (see fig. 2)
b	wing span, 4.00 ft
V	free-stream velocity, ft/sec
ρ	mass density of air, slugs/cu ft
δ_f	flap deflection relative to wing-chord plane, measured from flap-chord plane in a plane normal to hinge line (positive when trailing edge is down), deg
α	angle of attack of wing, deg
c	local wing chord, ft
c_f'	local flap chord, measured normal to flap leading edge, ft
y	lateral distance from plane of symmetry measured parallel to Y-axis, ft
z	vertical distance from wing-chord plane positive when above chord plane, ft (fig. 2(c))
l	distance of tail quarter-chord position rearward of the wing quarter-chord position, ft (fig. 2(c))
i_t	incidence of horizontal tail measured from wing-chord plane, deg

Subscripts:

max	maximum
t	horizontal tail

MODEL AND APPARATUS

The model was tested on a single-support strut in the Langley 300 MPH 7- by 10-foot wind tunnel. The aerodynamic forces and moments were measured on a six-component mechanical balance system.

The pointed wing (fig. 2(a) and table I) was essentially a flat steel plate 5/8 inch thick with beveled leading and trailing edges, having 60° sweep of the leading edge, -23.1° sweep of the trailing edge, and rounded tips. The thickness varied from 0.012c at the root to a maximum of 0.047c at 0.746b/2.

The double slotted flap arrangement tested (fig. 2(b) and tables II and III) consisted of a tapered flap constructed of steel with a wood leading edge and a tapered vane consisting of a steel spar with wood covering.

For the flap in the deflected position the leading edge of the vane was along the hinge line which was the 83-percent chord line and the inboard edge of the flap was skewed relative to the fuselage. With a flap deflection of 52.5° the inboard tip of the flap trailing edge was 5.36 inches from the plane of symmetry. For the undeflected position of the flap, relative movement between the vane and flap would be necessary to stow the vane; since stowage space for the vane was not provided in the construction of the model, the vane was removed for the undeflected-flap tests.

The horizontal-tail configurations and locations tested on the model are shown in figure 2(c). The 60° delta tail had an aspect ratio of 2.31 and was constructed of 1/4-inch aluminum. The aspect-ratio-3.06 straight tail had a taper ratio of 0.394 and was a double-wedge airfoil made of aluminum. The areas of the delta and straight tails were 16.1 percent and 11.6 percent of the wing area, respectively. Provisions were made for locating the tails at the different longitudinal positions by means of interchangeable afterbody sections (fig. 2(a)); positioning the tails above and below the wing chord line was accomplished by supporting the tail on 1/2-inch steel vertical struts.

The 60° delta vertical tail was constructed of 1/8-inch-thick aluminum and had an area which was 18.4 percent of the wing area (fig. 2(a)).

TESTS

The tests were made at a dynamic pressure of approximately 25 pounds per square foot corresponding to an airspeed of about 100 miles per hour. The corresponding Mach number was 0.13. Reynolds number based on the mean aerodynamic chord was approximately 2.7×10^6. The model was tested at angles of attack from -12° to 32°.

Data were obtained for flap deflections of 0°, 40°, 45°, 50°, 52.5°, 55°, 60°, and 65° for the model without a horizontal tail. Tests of the model with straight and delta horizontal tails were made at several tail incidences with flap deflections of 50° or 52.5° for the tail locations shown in figure 2(c). The parameters C_{n_β}, C_{Y_β}, and C_{l_β} were determined from tests at sideslip angles of $\pm 5^\circ$ for the model with tails off, with a delta vertical tail, and with a delta vertical and horizontal tail.

CORRECTIONS

Jet-boundary corrections, obtained by methods outlined in reference 7, have been applied to the angle of attack, the drag coefficient, the pitching-moment coefficient, and rolling-moment coefficient data.

Blocking corrections have been applied according to the method of reference 8. A buoyancy correction has been applied to the data to account for a longitudinal static-pressure gradient in the tunnel. The angles of attack have been corrected to account for airstream inclination.

RESULTS AND DISCUSSION

The data are presented in the following figures:

	Figure
Longitudinal aerodynamic characteristics:	
Effect of flap deflection, tail off	3
Effect of straight tail	4
Effect of delta tail	5
Lateral stability characteristics:	
Lateral stability parameters	6

Longitudinal Aerodynamic Characteristics

<u>Effect of double slotted flap deflection, tail off</u>.- For the flap-deflection range (40° to 52.5°), substantial increments of lift coefficient, which increased with flap deflection, were obtained throughout the lift-coefficient range to near $C_{L_{max}}$ with the $l = 1.56\bar{c}$ afterbody section (fig. 3). For flap deflections greater than 52.5°, flap effectiveness decreased with increase of flap deflection. Although a flap deflection of 52.5° produced about the maximum flap effectiveness, the largest value of $C_{L_{max}}$ (1.58) occurred for a flap deflection of 40°. (The value of $C_{L_{max}}$ for the model with flaps undeflected was approximately 1.20.) For flap deflections up to 55° the increment of lift coefficient for a given flap deflection varied only slightly throughout the lift-coefficient range to near $C_{L_{max}}$ (similar to the delta wing with extended double slotted flaps of ref. 5). With a flap deflection of 52.5° the lift coefficient at an angle of attack of 0° for the pointed wing was 0.66 and $C_{L_{max}}$ was 1.53. For the delta wing of reference 4 with a flap deflection of 52°, the value of the lift coefficient at an angle of attack of 0° was 0.89 and $C_{L_{max}}$ was 1.53. It should be noted that the flap-wing area ratio (0.1191) of the present investigation was smaller than that of reference 4 (0.1483) and accounts largely for the lower lift coefficient at an angle of attack of 0°. An angle of attack of about 23° was required for the plain wing to obtain a lift coefficient of 1.0, whereas an angle of attack of about 7° was required to obtain the same lift coefficient with a flap deflection of 52.5°.

At lift coefficients above 0.65 the lift-drag ratio for the wing with double slotted flaps deflected 52.5° was higher than that for the plain wing.

With the exception of some neutral stability over the high lift-coefficient range (fig. 3), the tail-off pitching-moment curves of the present investigation for flap-deflection angles up to 52.5° generally remain stable up to the stall. Pitching-moment characteristics exhibited undesirable nonlinearity when flap deflections were increased above 52.5°, corresponding to flap deflections for which flap effectiveness decreased (fig. 3(b)). In the delta-wing investigation of reference 4, instability occurred with the tail-off configuration for all flap deflections tested. For lift coefficients up to the maximum, the tail-off pitching-moment curves of the present investigation had less diving moments than for the corresponding lift-coefficient values of reference 5.

<u>Effect of straight tail on the longitudinal stability and control</u>.- A longitudinally stable configuration with flaps deflected occurred with location of the straight tail rearward and below the chord line extended

($l = 1.56\bar{c}$, $z = -0.20\bar{c}$) and longitudinal instability occurred for the model with rearward position of the tail above the chord line extended (fig. 4(a)), similar to the effect of straight-tail location of reference 5. The high forward locations of the straight tail ($l = 1.15\bar{c}$, $z = 0.60\bar{c}$ and $l = 0.75\bar{c}$, $z = 0.60\bar{c}$) resulted in configurations that remained longitudinally stable to slightly below the stall. However, when located at the low favorable position for longitudinal stability or at the high forward positions, the present straight tail would be unable to provide longitudinal trim throughout the lift-coefficient range as indicated by the tail-incidence data of figures 4(b) and 4(c).

Effect of the delta tail on the longitudinal stability and control.- For tail location rearward and below the chord line extended ($l = 1.56\bar{c}$, $z = -0.20\bar{c}$) longitudinal stability also occurred with the delta tail for the model with flaps deflected (fig. 5(a)). No other investigation was made with the delta tail at this tail length since it is believed that the stability characteristics would be similar to that found for the straight tail and the results of references 4 and 5. Tail-incidence data of figure 5(b) and the tail-off data of figure 3 indicate that, with a high forward location of the delta tail ($l = 0.75c$; $z = 0.60c$), longitudinal trim would be unattainable throughout the lift-coefficient range. From consideration of the similarity of the pitching-moment curves of the present investigation to those of reference 4 it is believed that longitudinal trim could be obtained throughout the lift-coefficient range with the delta tail located rearward and below the chord line extended ($l = 1.56\bar{c}$, $z = -0.20\bar{c}$).

Lateral Stability Characteristics

Yawing moment and side force due to sideslip.- The delta vertical tail provided static directional stability of the model with horizontal tail off and flaps deflected 52.5° except at high lift coefficients, where large reversals in both C_{n_β} and C_{Y_β} occurred (fig. 6). Addition of the delta horizontal tail further increased the static directional stability up to a lift coefficient of 1.06.

Rolling moment due to sideslip.- Positive effective dihedral $-C_{l_\beta}$ (fig. 6) increased with increase of lift coefficient throughout most of the lift-coefficient range for the tails-off configuration with flaps deflected 52.5°; however, a reduction in the effective dihedral occurred at approximately a lift coefficient of 1.1. Employing the delta vertical tail generally resulted in additional positive dihedral, the increment of which decreased with increase of lift coefficient. The effect of the delta horizontal tail on the rolling moment of the tails-on configuration was small.

CONCLUSIONS

A low-speed investigation to determine the longitudinal characteristics of a thin aspect-ratio-1.85, pointed-wing—fuselage configuration with double slotted flaps including the effects of a straight and a delta horizontal tail on the longitudinal stability and the effect of a delta vertical tail on the static lateral stability indicates the following conclusions:

1. The angle of attack required to obtain a given lift coefficient was considerably reduced with deflection of the double slotted flap. An angle of attack of about 23° was required for the plain wing to obtain a lift coefficient of 1.0, whereas an angle of attack of about 7° was required to obtain the same lift coefficient with a flap deflection of 52.5°. Most of the lift-coefficient increment with flap deflection held throughout the angle-of-attack range to the stall. With a flap deflection of 52.5° the lift coefficient at an angle of attack of 0° was 0.66 and the maximum lift coefficient was 1.53.

2. For longitudinal stability of the model with the double slotted flaps deflected, the satisfactory location for a straight or delta horizontal tail was rearward and below the wing chord line extended.

3. The delta vertical tail provided static directional stability of the model with double slotted flaps deflected 52.5° except at high lift coefficients where large reversals in the variation of yawing moment and lateral force with sideslip occurred. The delta vertical tail generally increased effective dihedral of the model.

Langley Aeronautical Laboratory,
National Advisory Committee for Aeronautics,
Langley Field, Va., April 3, 1956.

REFERENCES

1. MacLeod, Richard G.: A Preliminary Low-Speed Wind-Tunnel Investigation of a Thin Delta Wing Equipped With a Double and a Single Slotted Flap. NACA RM L51J26, 1952.

2. Riebe, John M., and MacLeod, Richard G.: Low-Speed Wind-Tunnel Investigation of a Thin 60° Delta Wing With Double Slotted, Single Slotted, Plain, and Split Flaps. NACA RM L52J29, 1953.

3. Riebe, John M.: The Effects of Fuselage Size on the Low-Speed Longitudinal Aerodynamic Characteristics of a Thin 60° Delta Wing With and Without a Double Slotted Flap. NACA RM L52L29a, 1953.

4. Riebe, John M., and Graven, Jean C., Jr.: Low-Speed Investigation of the Effects of Location of a Delta Horizontal Tail on the Longitudinal Stability and Control of a Fuselage and Thin Delta Wing With Double Slotted Flaps Including the Effects of a Ground Board. NACA RM L53H19a, 1953.

5. Riebe, John M., and Graven, Jean C., Jr.: Low-Speed Investigation of the Effects of Location of a Delta and a Straight Tail on the Longitudinal Stability and Control of a Thin Delta Wing With Extended Double-Slotted Flaps. NACA RM L53J26, 1954.

6. Smith, Donald W., and Reed, Verlin D.: Subsonic Static Longitudinal Stability and Control Characteristics of a Wing-Body Combination Having a Pointed Wing of Aspect Ratio 2 With Constant-Percent-Chord Trailing-Edge Elevons. NACA RM A53C20, 1953.

7. Gillis, Clarence L., Polhamus, Edward C., and Gray, Joseph L., Jr.: Charts for Determining Jet-Boundary Corrections for Complete Models in 7- by 10-Foot Closed Rectangular Wind Tunnels. NACA WR L-123, 1945. (Formerly NACA ARR L5G31.)

8. Herriot, John G.: Blockage Corrections for Three-Dimensional-Flow Closed-Throat Wind Tunnels, With Consideration of the Effect of Compressibility. NACA Rep. 995, 1950. (Supersedes NACA RM A7B28.)

TABLE I

PHYSICAL CHARACTERISTICS OF THE TEST MODEL

Wing:	
Span, ft	4.00
Aspect ratio	1.85
Thickness of flat plate (maximum thickness ratio, 0.047), in.	5/8
Leading-edge sweep, deg	60.0
Trailing-edge sweep, deg	-23.1
Area, sq ft	8.63
Mean aerodynamic chord, ft	2.88
Leading-edge bevel angle, deg	6.8
Trailing-edge bevel angle, deg	7.9
Taper ratio	0
Vane:	
Span, ft	2.98
Chord, percent wing chord	5.40
Chord, percent flap chord	27.32
Flap:	
Span, ft	2.98
Chord, percent wing chord	19.76
Exposed area, sq ft	1.03
Area, percent wing area	11.91
Trailing-edge bevel angle, deg	7.9
Delta horizontal tail:	
Span, ft	1.79
Aspect ratio	2.31
Thickness of flat plate (maximum thickness ratio, 0.045), in.	1/4
Leading-edge sweep, deg	60.0
Area, sq ft	1.39
Area, percent wing area	16.1
Mean aerodynamic chord, ft	1.03
Leading-edge bevel angle, deg	6.0
Trailing-edge bevel angle, deg	7.3
Taper ratio	0
Straight horizontal tail:	
Span, ft	1.75
Aspect ratio	3.06
Taper ratio	0.394
Root thickness ratio	0.045
Leading-edge sweep, deg	23.1
Area, sq ft	1.0
Area, percent wing area	11.6
Mean aerodynamic chord, ft	0.61
Delta vertical tail:	
Aspect ratio	1.15
Thickness of flat plate, in.	1/8
Leading-edge sweep, deg	60.0
Area, sq ft	1.6
Area, percent wing area	18.4
Mean aerodynamic chord, ft	1.57

TABLE II.- ORDINATES OF THE VANE

(Ordinates are given in percent chord)

Station	Upper surface	Lower surface
0	0	0
2.5	5.2	-5.2
5.0	7.2	-6.7
10.0	10.2	-8.5
20.0	13.6	-9.2
30.0	15.0	-7.2
40.0	14.8	-4.4
50.0	13.5	-2.7
60.0	11.1	-2.0
70.0	7.5	-2.3
100.0	-9.7	-9.7

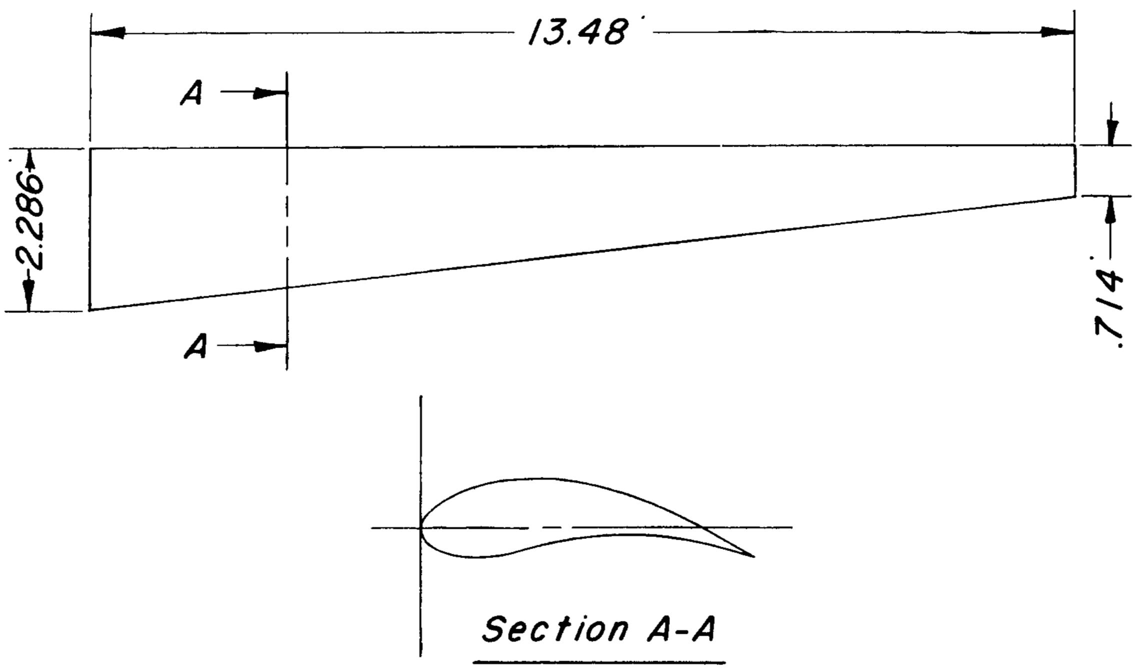

TABLE III.- ORDINATES OF THE TRAILING-EDGE FLAP

(All dimensions are in inches.)

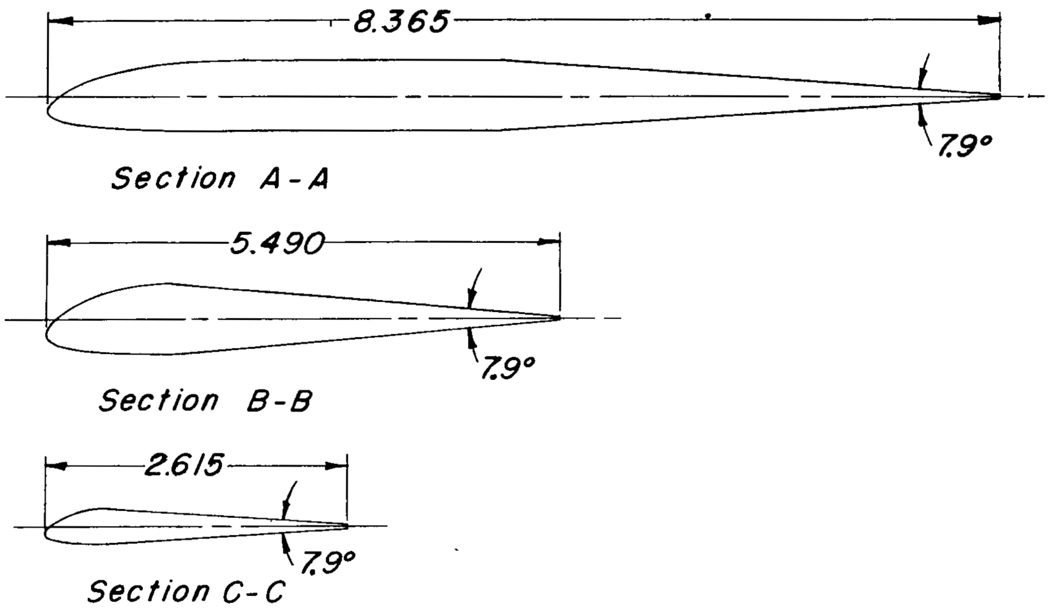

Ordinates of the leading edge of the trailing-edge Flap

Station	Upper surface	Lower surface
Section A-A		
0	-0.150	-0.150
.152	.010	- .250
.305	.080	- .270
.610	.180	- .290
.914	.250	- .300
1.219	.300	- .310
1.676	.312	- .312
Section B-B		
0	-0.150	-0.150
.100	.010	- .250
.200	.080	- .270
.400	.180	- .290
.600	.250	- .300
.800	.300	- .310
1.100	.312	- .312
Section C-C		
0	-0.075	-0.075
.048	.005	- .124
.095	.040	- .134
.191	.090	- .144
.286	.124	- .149
.381	.149	- .154
.524	.154	- .154

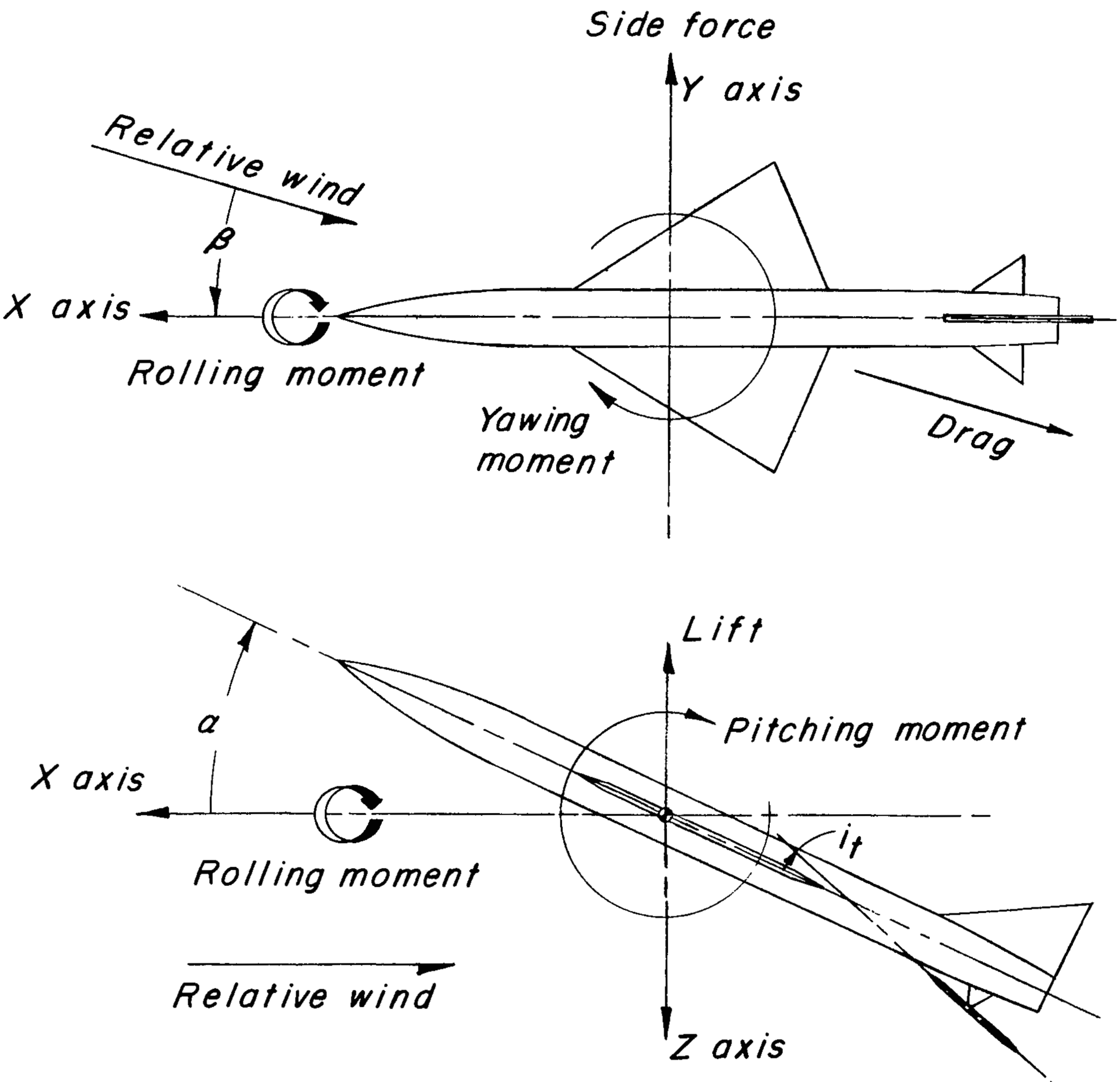

Figure 1.- System of stability axes. Positive values of forces, moments, and angles are indicated by arrows.

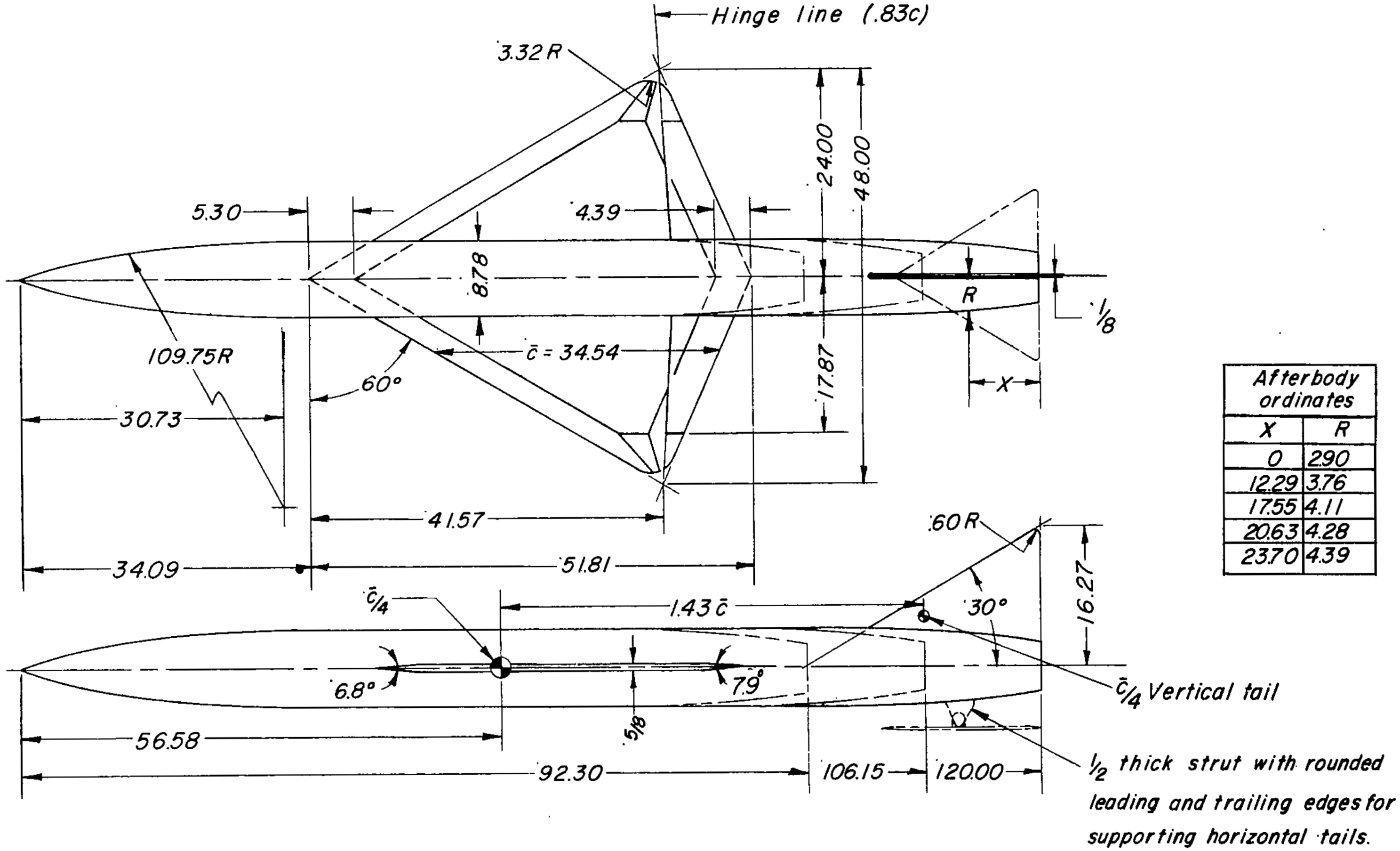

Afterbody ordinates	
X	R
0	2.90
12.29	3.76
17.55	4.11
20.63	4.28
23.70	4.39

(a) Details of fuselage, wing, and vertical tail.

Figure 2.- General arrangement of the model. (All dimensions are in inches except where noted.)

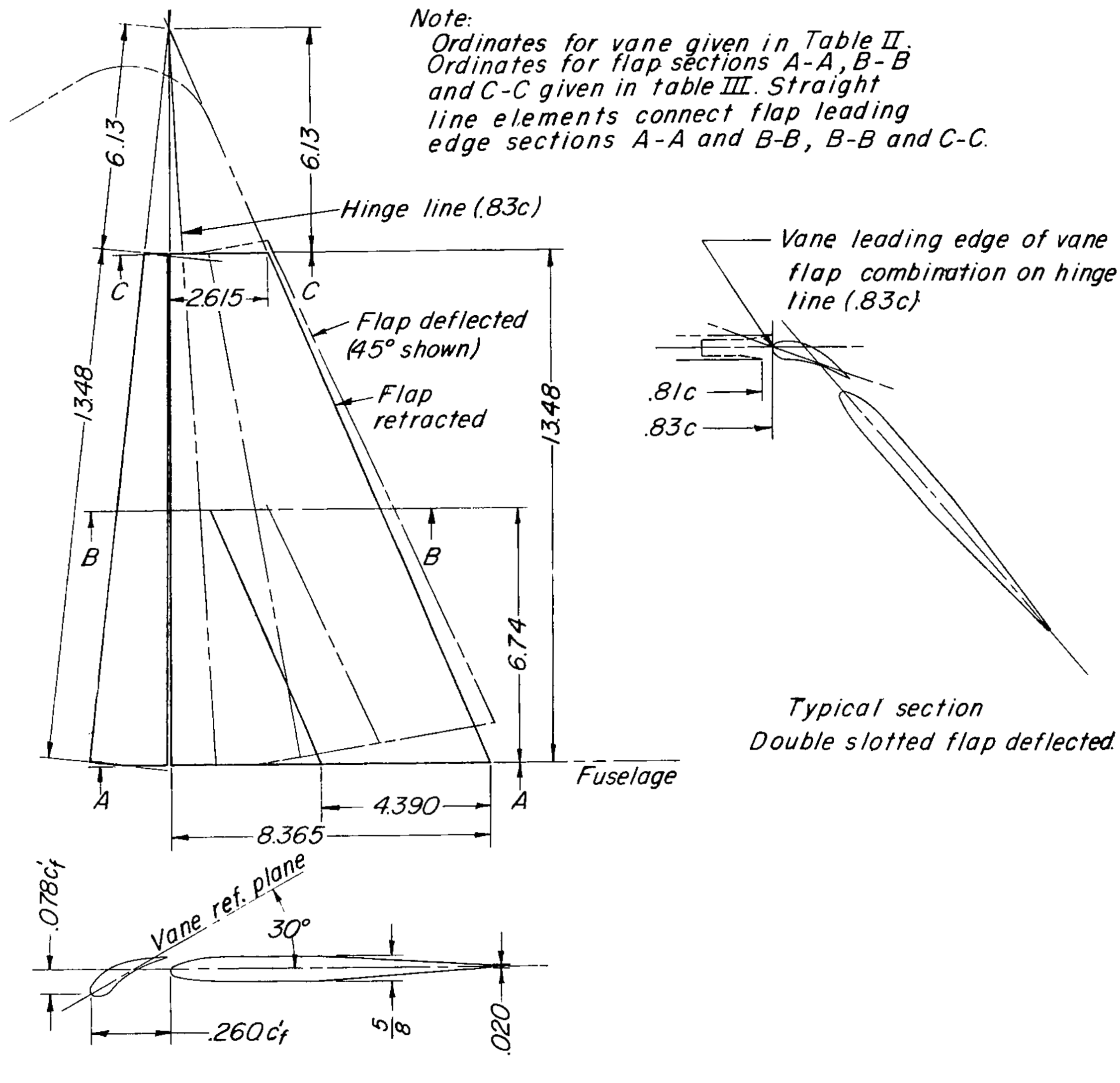

Vane flap construction details and assembly.

(b) Details of double slotted flap.

Figure 2.- Continued.

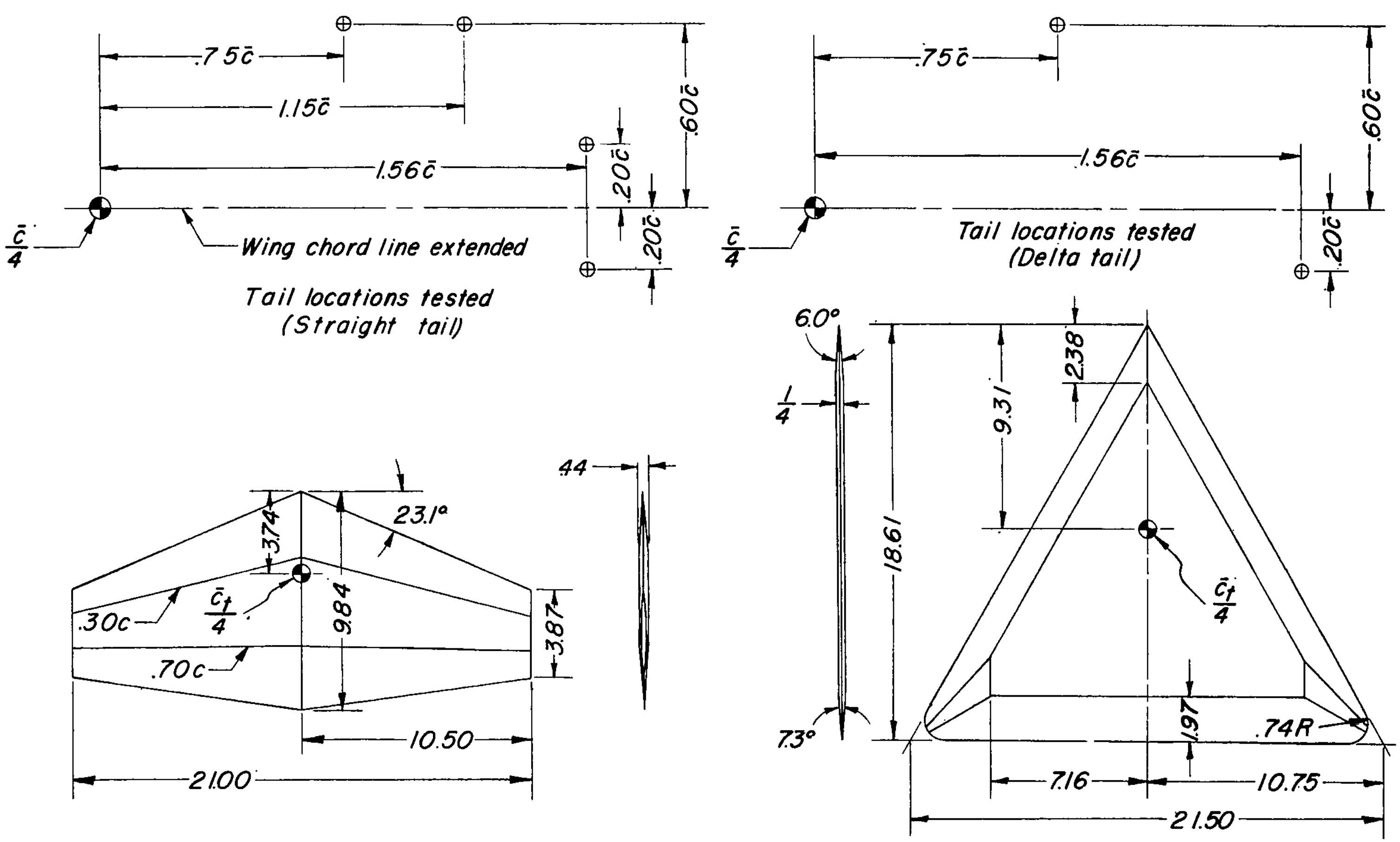

(c) Details of horizontal tails and tail locations tested.

Figure 2.- Concluded.

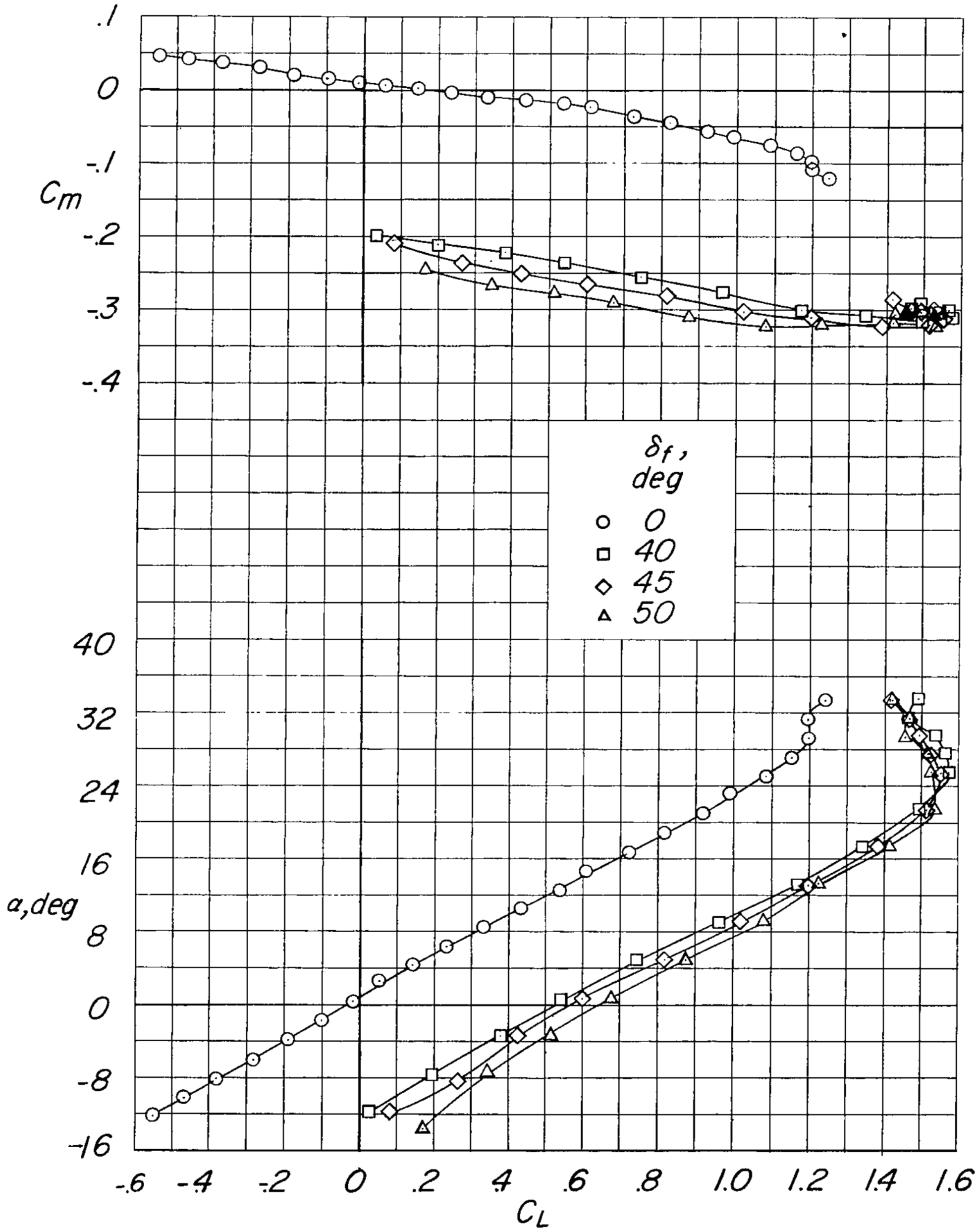

(a) $\delta_f = 0^{\circ}, 40^{\circ}, 45^{\circ}$, and 50°.

Figure 3.- Effect of deflection of the double slotted flaps on the longitudinal aerodynamic characteristics of the aspect-ratio-1.85 pointed-wing—fuselage configuration. Tails off; fuselage with $l = 1.56\bar{c}$ afterbody section.

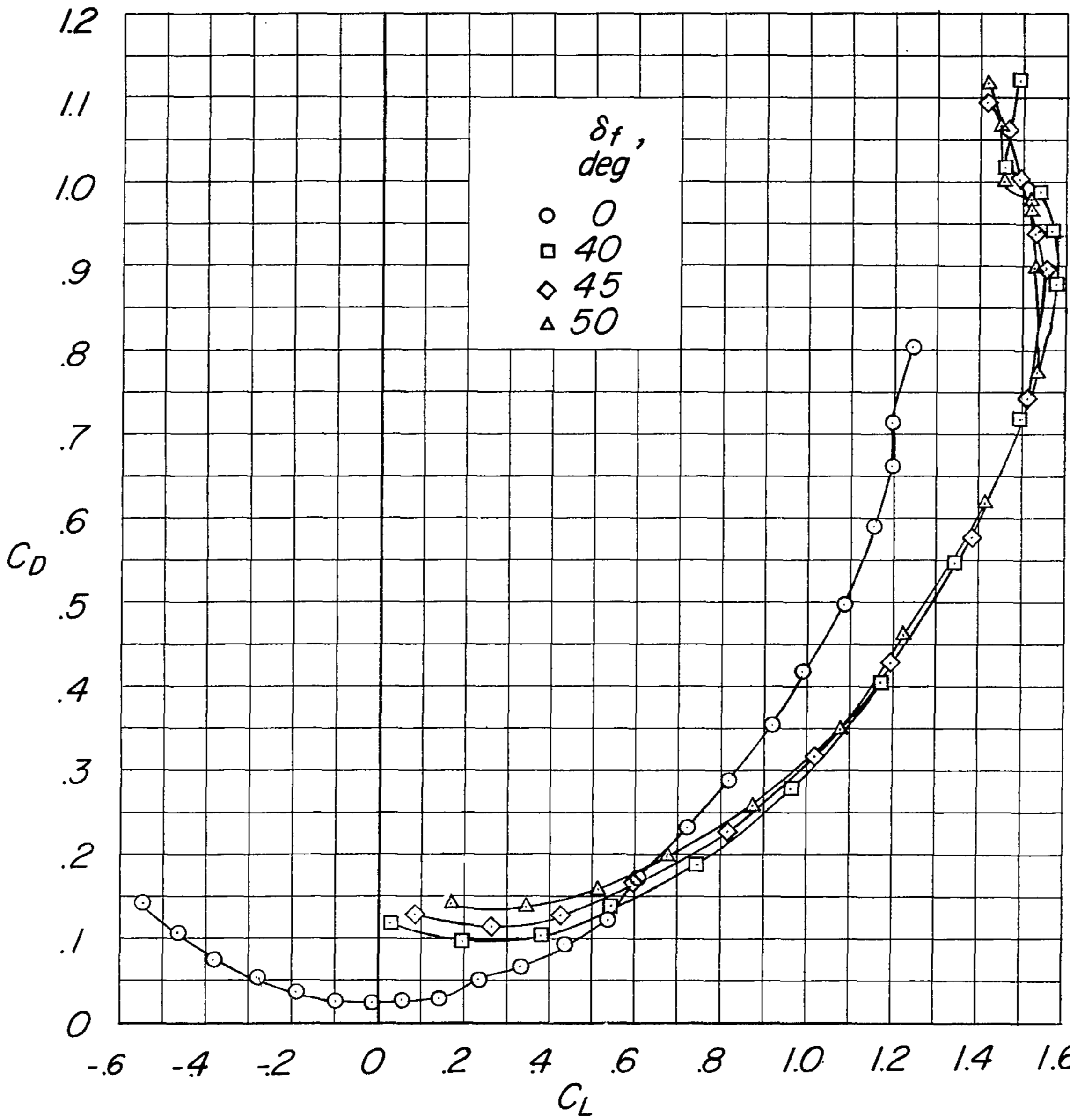

(a) Concluded.

Figure 3.- Continued.

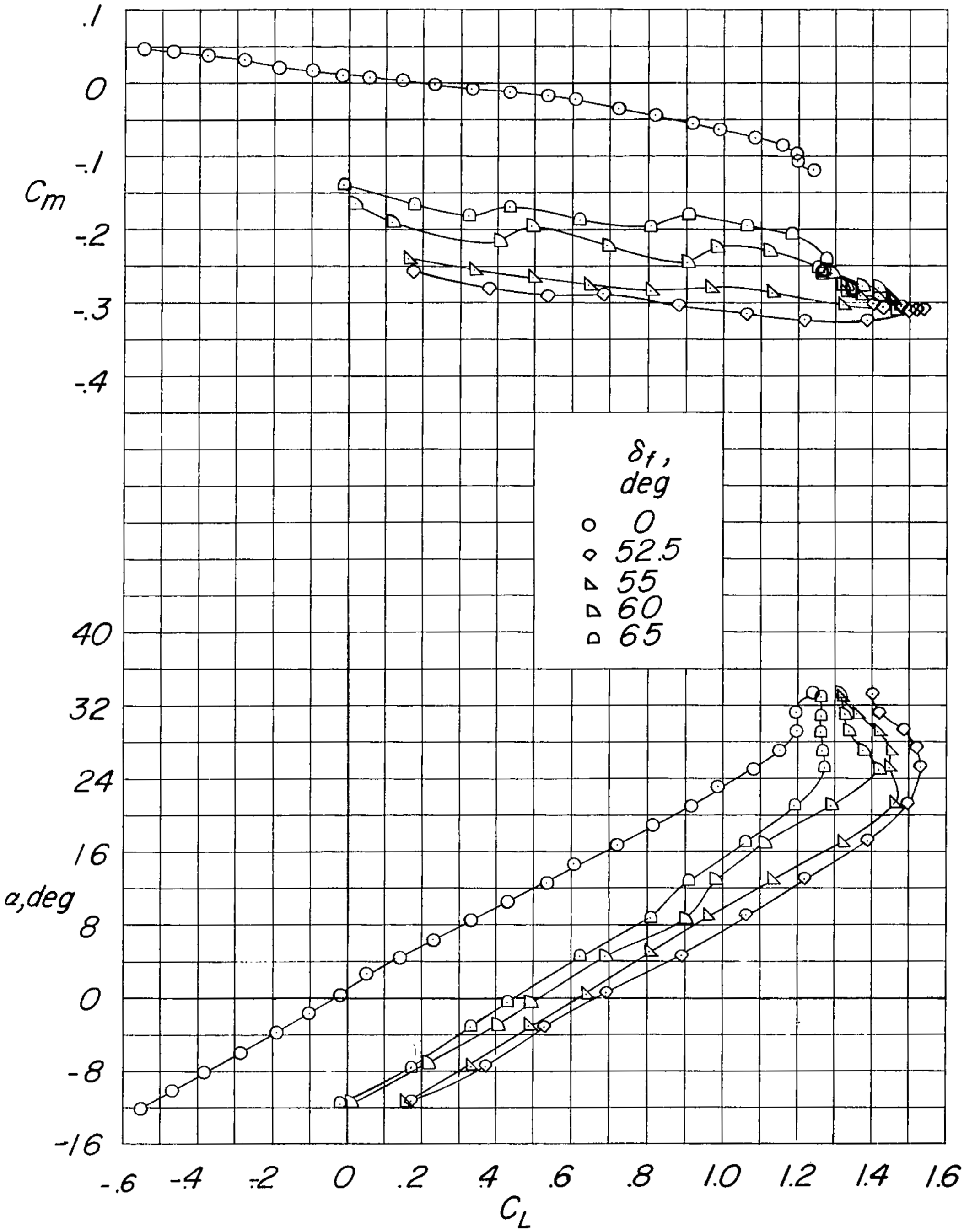

(b) $\delta_f = 0^{\circ}$, 52.5°, 55°, 60°, and 65°.

Figure 3.- Continued.

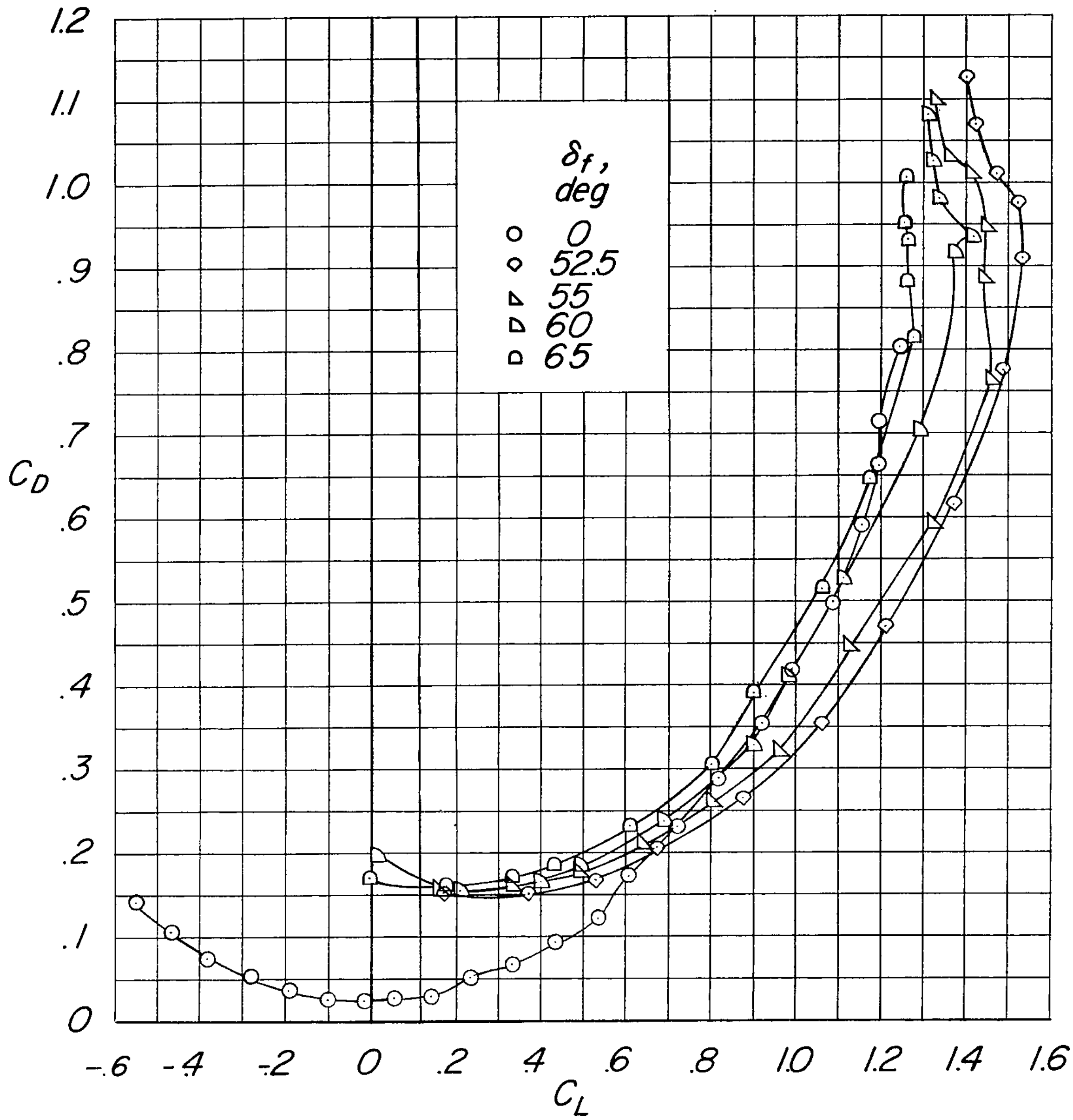

(b) Concluded.

Figure 3.- Concluded.

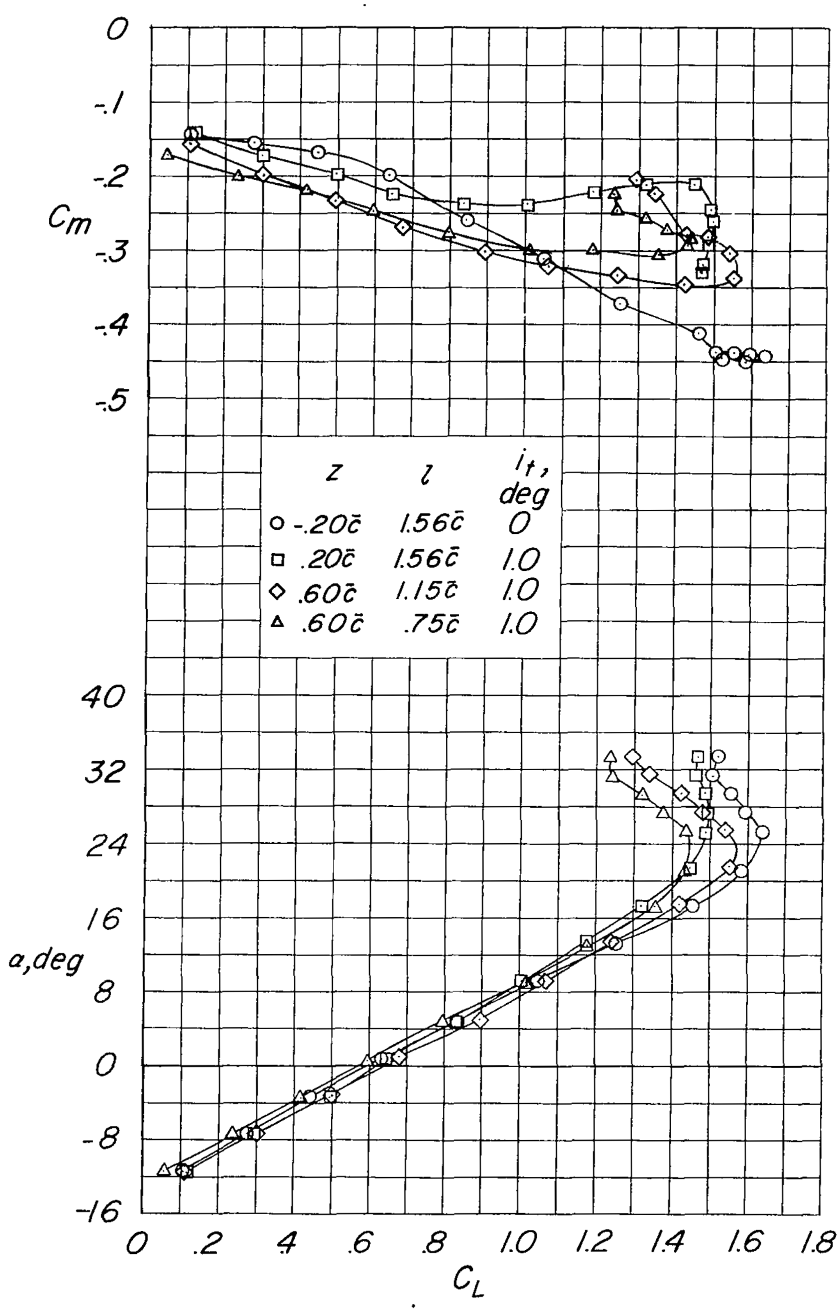

(a) Effect of tail location.

Figure 4.- Effect of the straight horizontal tail on the longitudinal aerodynamic characteristics of the aspect-ratio-1.85 pointed-wing—fuselage configuration with double slotted flaps deflected 50°.

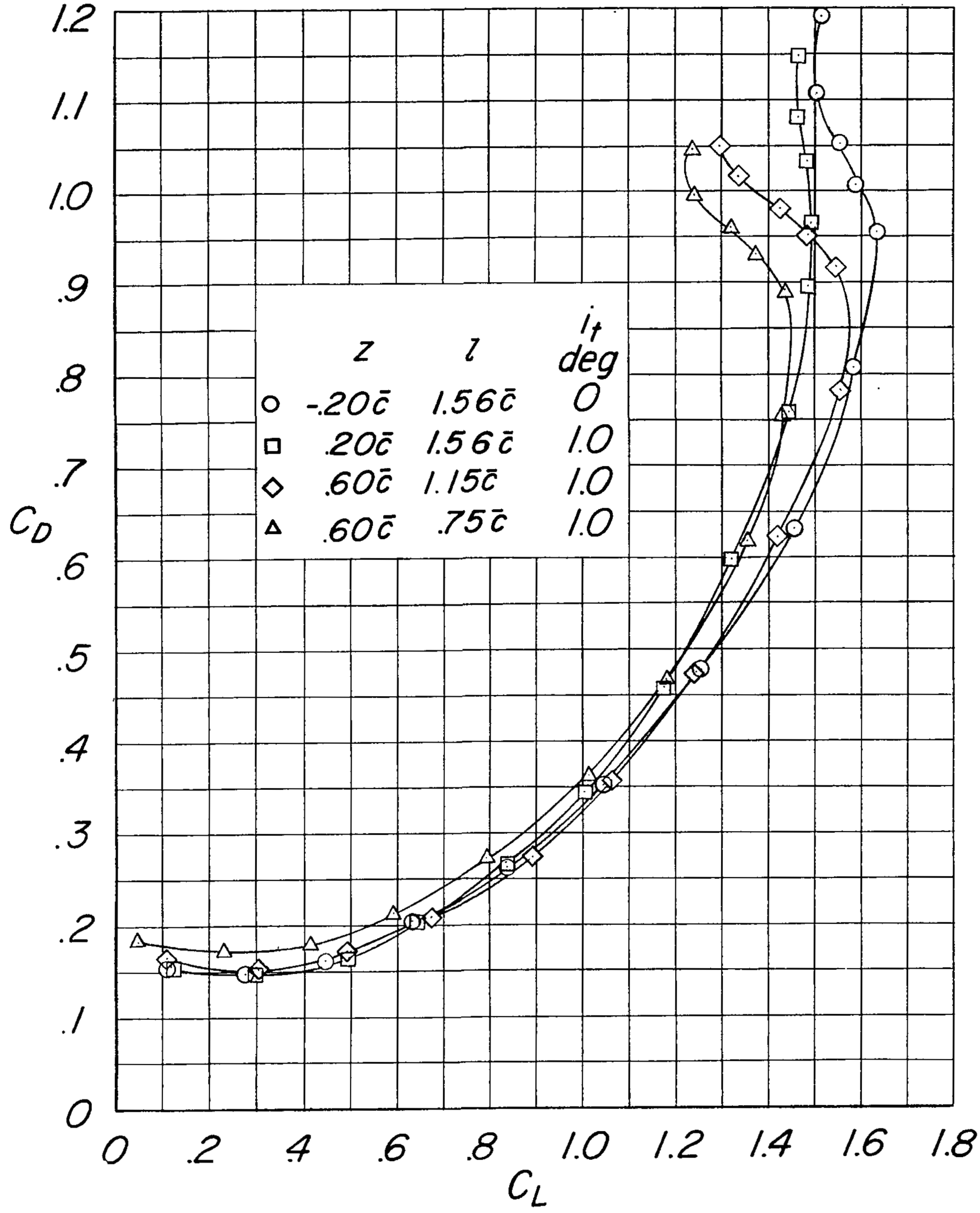

(a) Concluded.

Figure 4.- Continued.

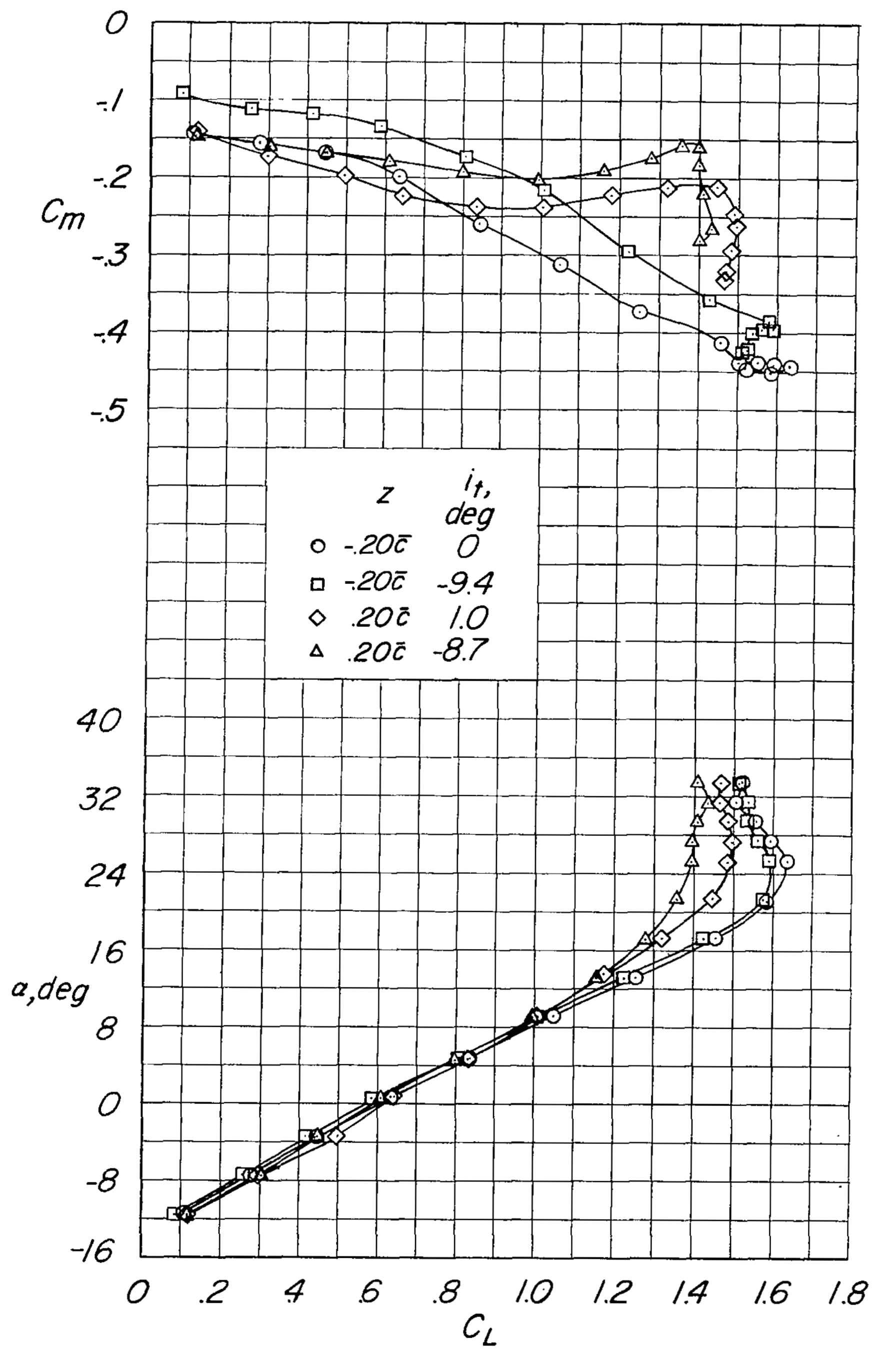

(b) Effect of incidence. $l = 1.56\bar{c}$.

Figure 4.- Continued.

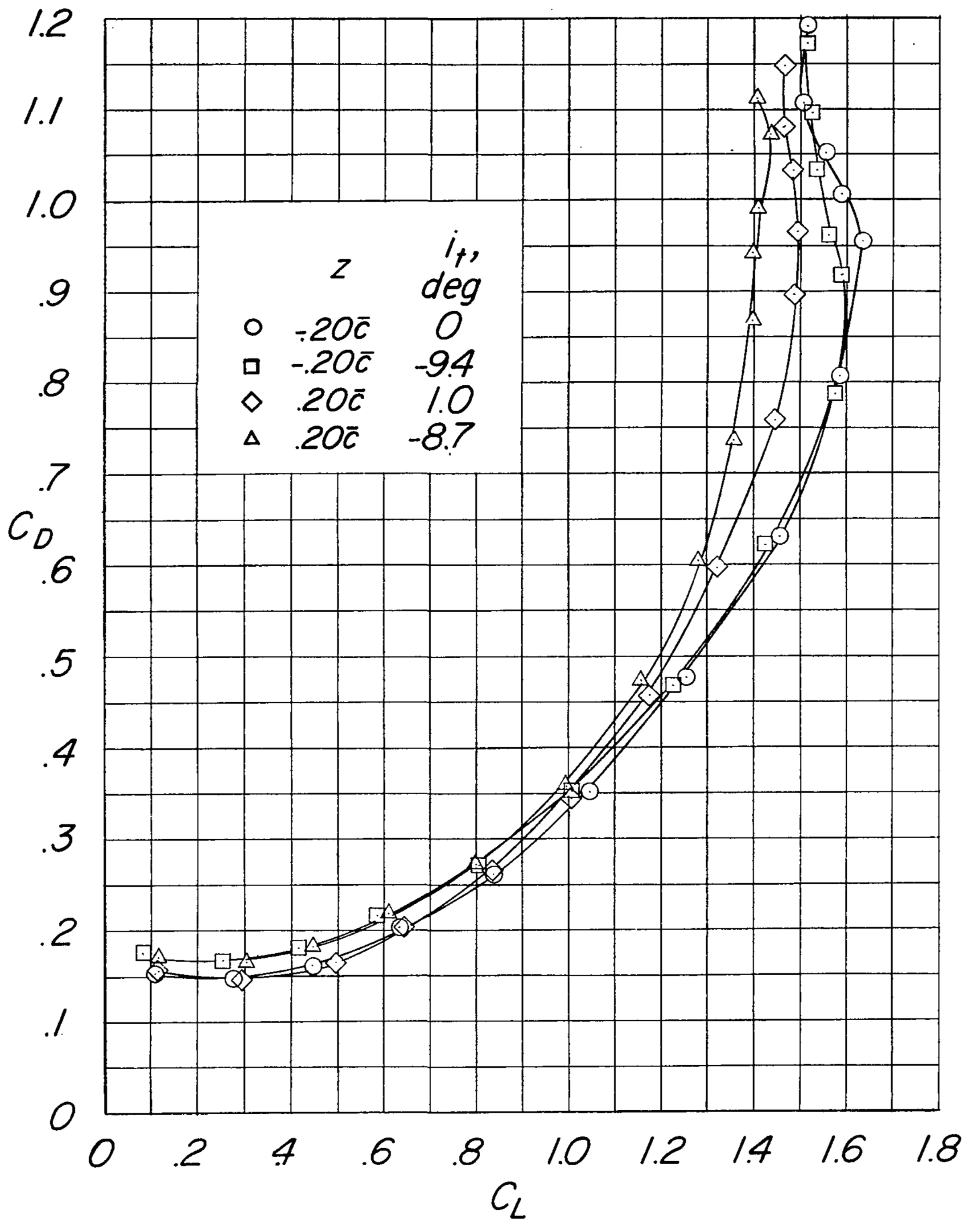

(b) Concluded.

Figure 4.- Continued.

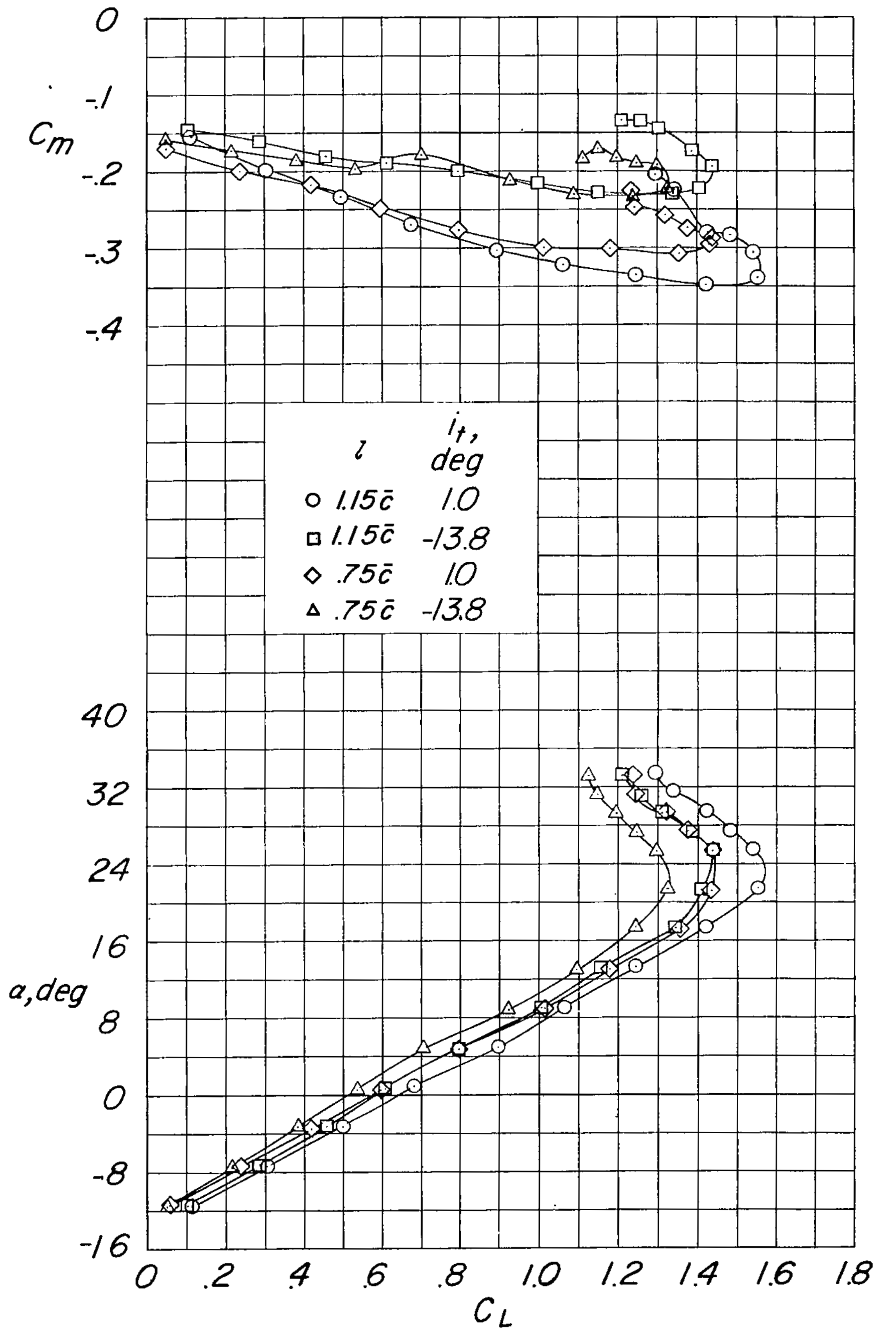

(c) Effect of incidence. z = 0.60c̄.

Figure 4.- Continued.

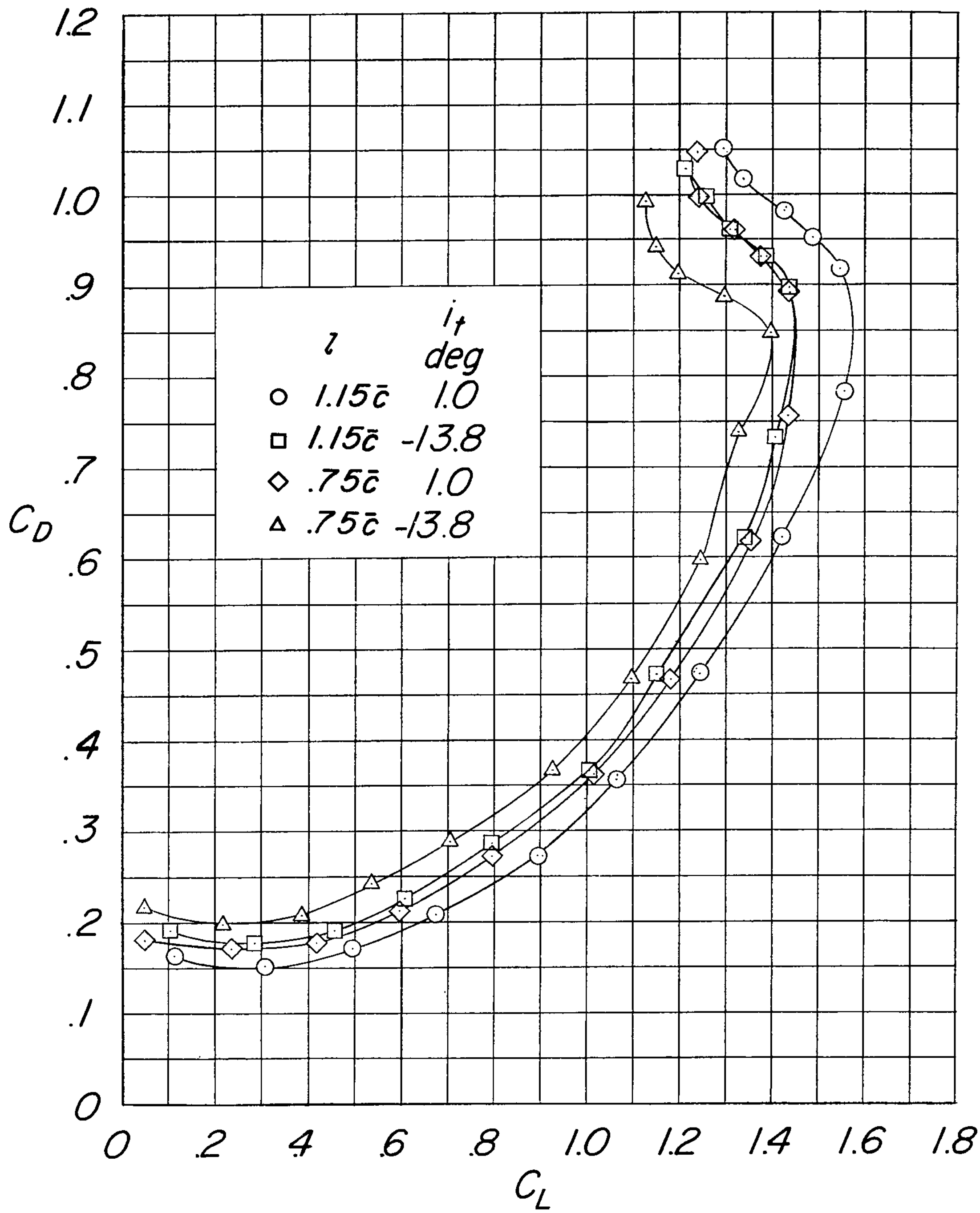

(c) Concluded.

Figure 4.- Concluded.

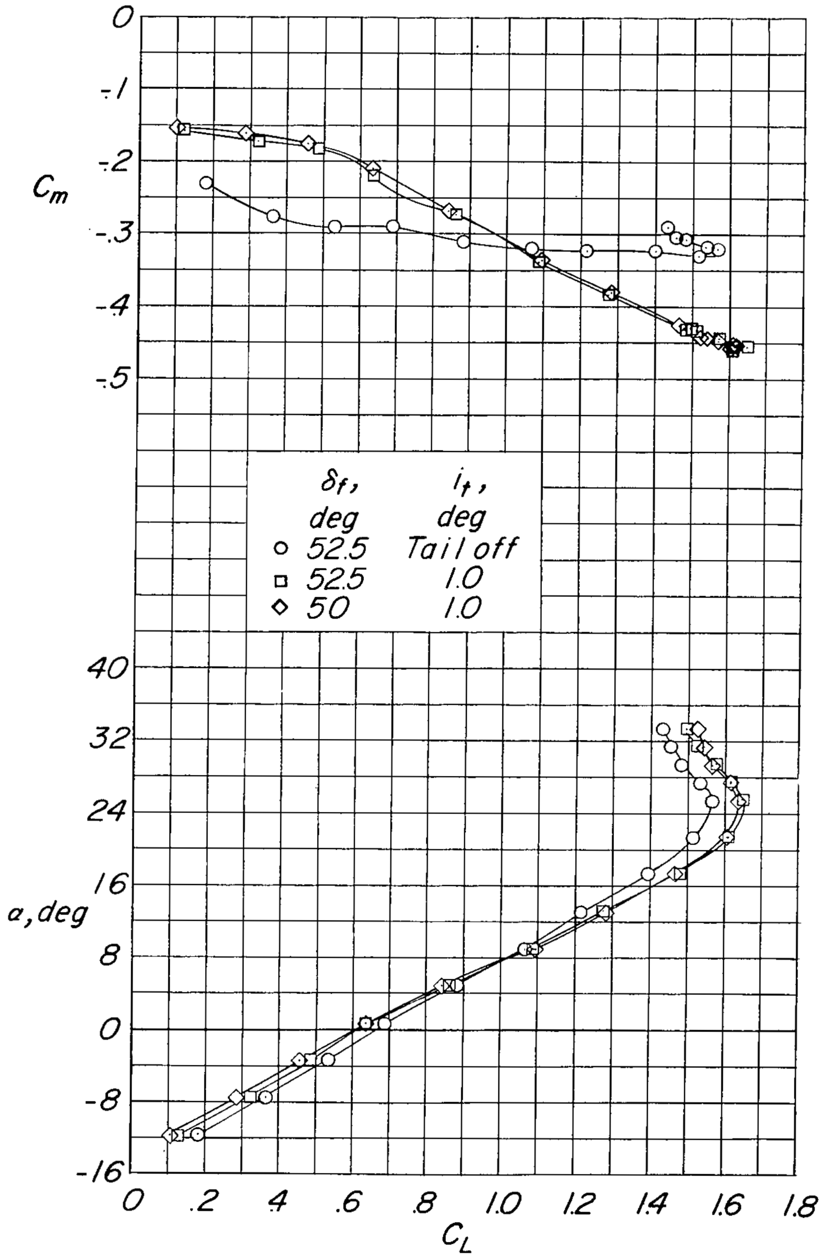

(a) $l = 1.56\bar{c}$; $z = -0.20\bar{c}$.

Figure 5.- Effect of the 60° delta horizontal tail on the longitudinal aerodynamic characteristics of the aspect-ratio-1.85 pointed-wing—fuselage with double slotted flaps deflected. (Fig. 5(a), vertical tail on; fig. 5(b), vertical tail off.)

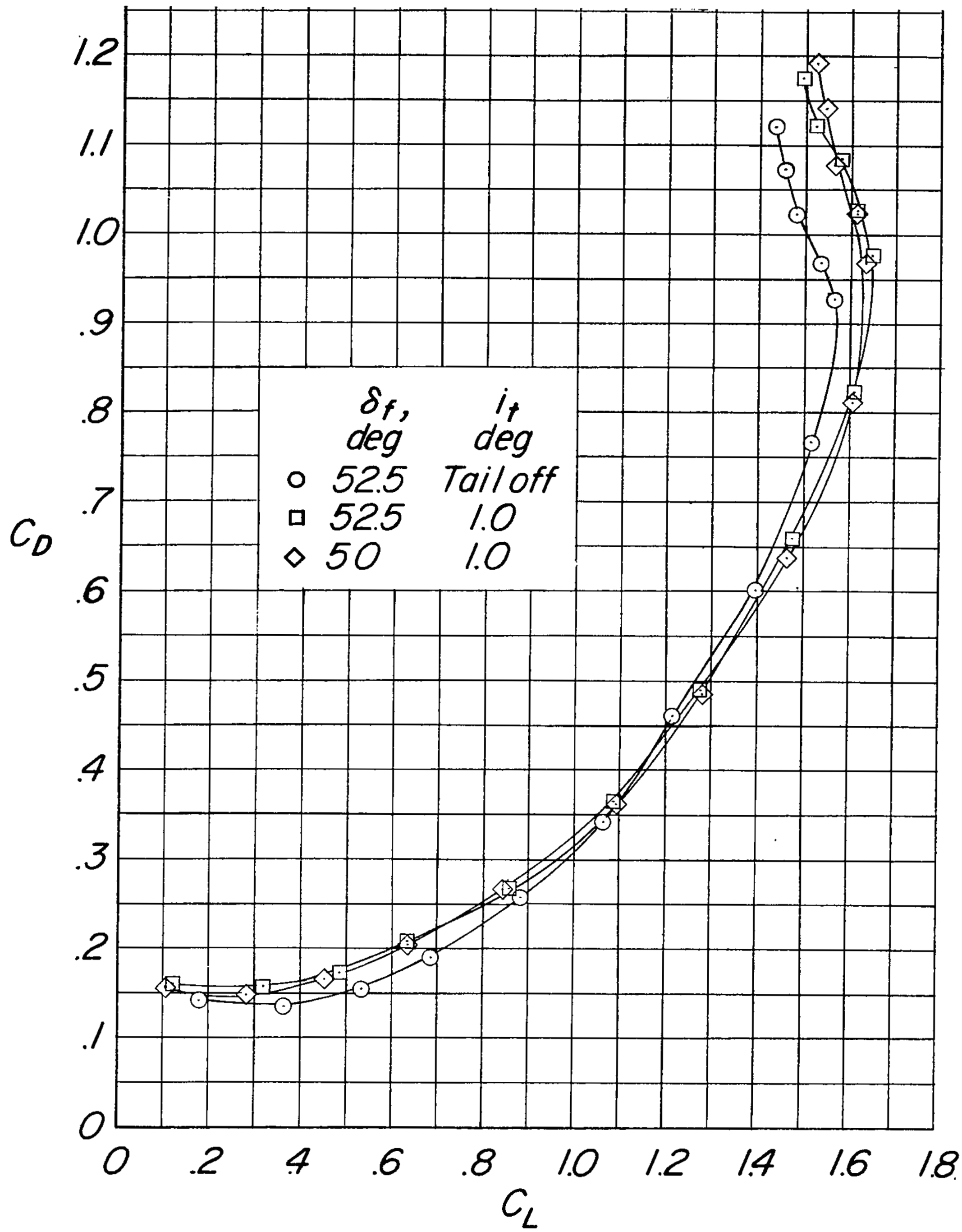

(a) Concluded.

Figure 5.- Continued.

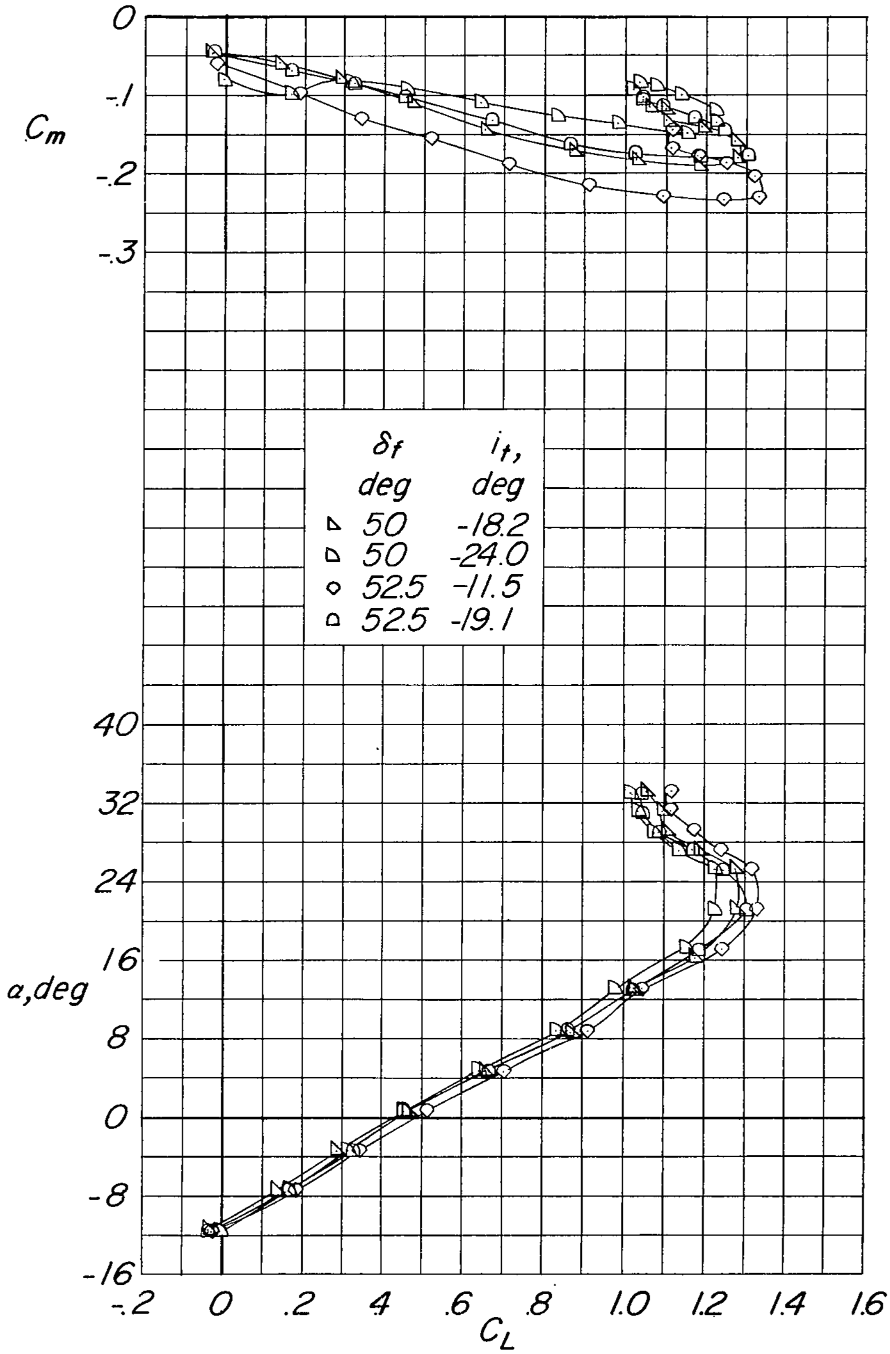

(b) $l = 0.75\bar{c}$; $z = 0.60\bar{c}$.

Figure 5.- Continued.

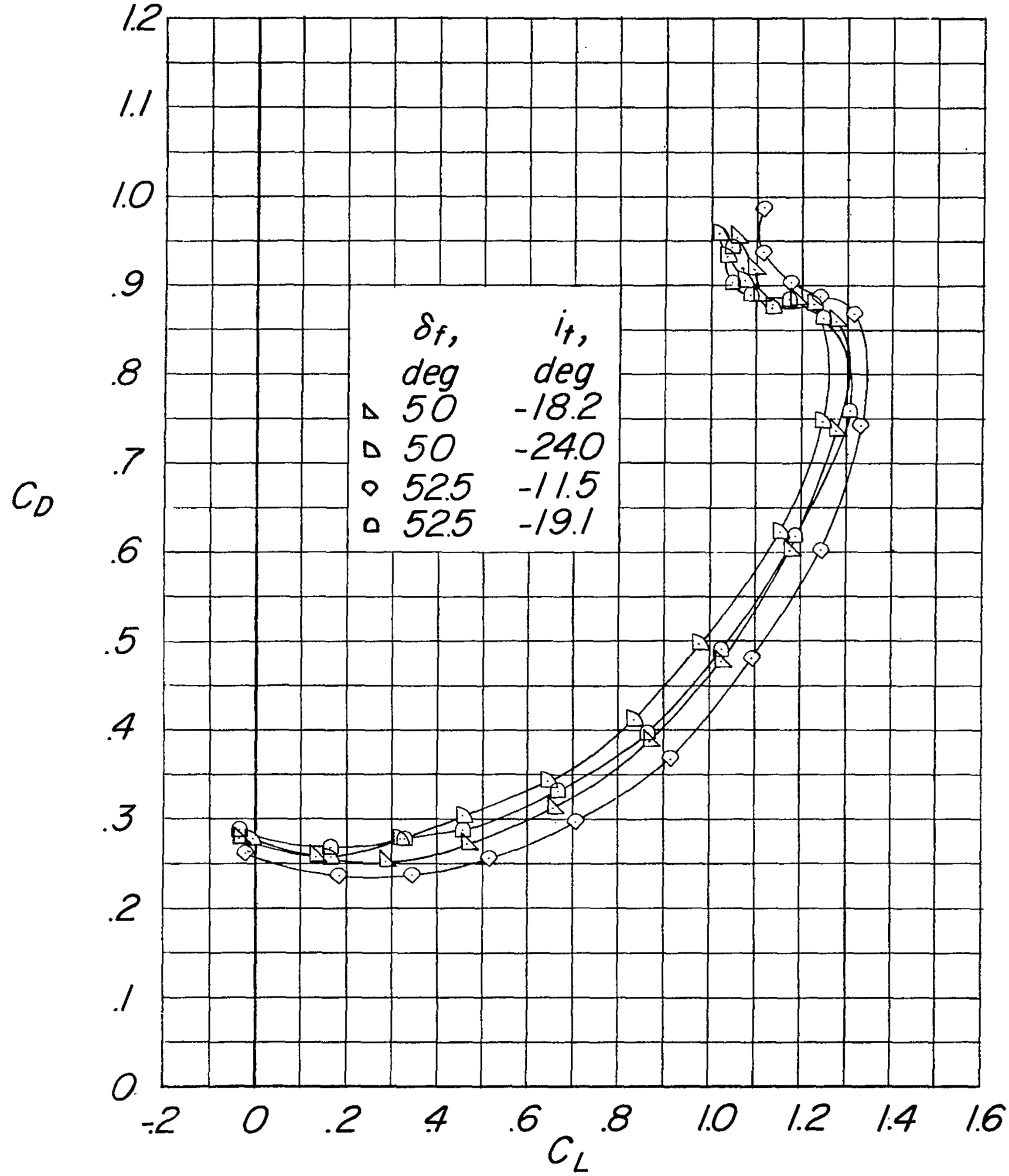

(b) Concluded.

Figure 5.- Concluded.

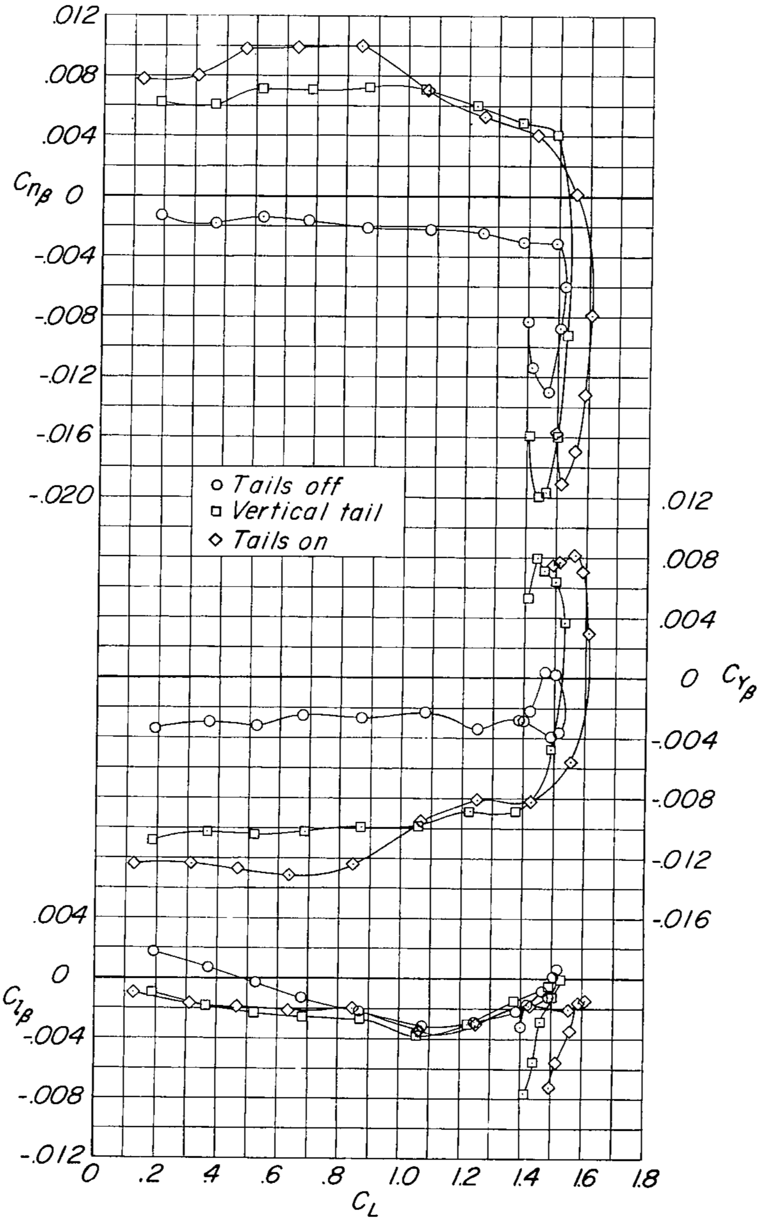

Figure 6.- Variation of the lateral stability parameters C_{n_β}, C_{Y_β}, and C_{l_β} with C_L of the aspect-ratio-1.85 pointed-wing—fuselage configuration, double slotted flaps deflected 52.5°, with tails off, with a delta vertical tail, and with delta vertical and horizontal tails. Vertical tail, $l = 1.43\bar{c}$; horizontal tail, $l = 1.56\bar{c}$; $z = -0.20\bar{c}$.

[redacted]

[redacted]

[redacted]